

Jets in pp at NNLO

João Pires*

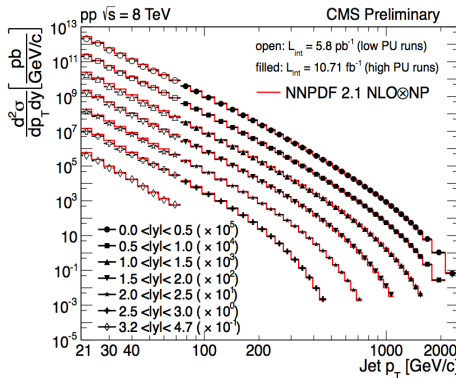
Universita di Milano-Bicocca and INFN, Sezione di Milano-Bicocca

PSR14 - Parton Showers, Event Generators and Resummation 2014
10-12 June 2014 Münster

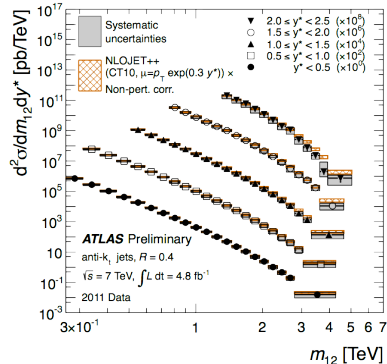
* in collaboration with J.Currie, A.Gehrmann-De Ridder, T.Gehrmann, N.Glover

Inclusive jet and dijet cross sections

- look at the **production** of jets of hadrons with large **transverse energy** in
 - inclusive jet events $pp \rightarrow j + X$
 - exclusive dijet events $pp \rightarrow 2j$
- **cross sections** measured as a function of the jet p_T , rapidity y and dijet **invariant mass** m_{jj} in **double differential form**

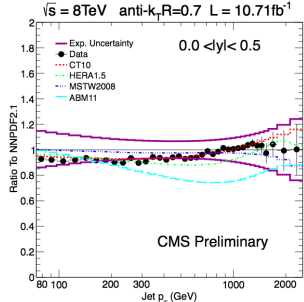
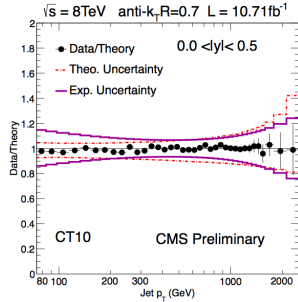


(CMS-PAS-SMP-12-012)



(ATLAS-CONF-2012-021)

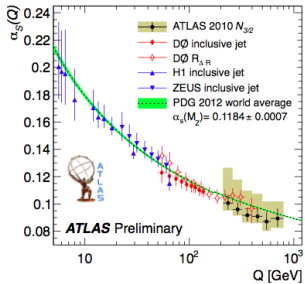
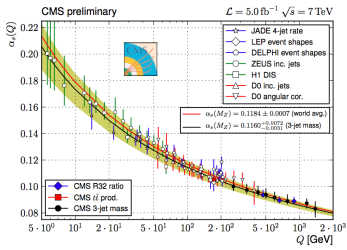
Inclusive jet cross section



Motivation for NNLO

- experimental uncertainties at high- p_T smaller than theoretical → need pQCD predictions to NNLO accuracy
- collider jet data can be used to constrain parton distribution functions
- size of NNLO correction important for precise determination of PDF's
- inclusion of jet data in NNLO parton distribution fits requires NNLO corrections to jet cross sections

Inclusive jet cross section



Motivation for NNLO

- experimental uncertainties at high- p_T smaller than theoretical → need pQCD predictions to NNLO accuracy
- collider jet data can be used to constrain parton distribution functions
- size of NNLO correction important for precise determination of PDF's
- inclusion of jet data in NNLO parton distribution fits requires NNLO corrections to jet cross sections
- α_s determination from hadronic jet observables limited by theoretical uncertainty due to scale choice

inclusive jet and dijet cross sections

State of the art:

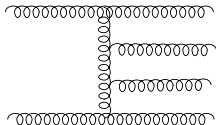
- dijet production is completely known in NLO QCD [Ellis, Kunszt, Soper '92], [Giele, Glover, Kosower '94], [Nagy '02]
- NLO+Parton shower [Alioli, Hamilton, Nason, Oleari, Re '11]
- approximate NNLO threshold corrections [Kidonakis, Owens '00], [Florian, Hinderer, Mukherjee, Ringer, Vogelsang '13]

Goal:

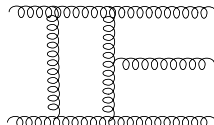
- obtain the jet cross sections at NNLO exact accuracy in **double differential** form

$$\frac{d^2\sigma}{dp_T dy} \quad \frac{d^2\sigma}{dm_{jj} dy^*}$$

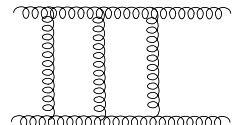
$pp \rightarrow 2j$ at NNLO: gluonic contributions



$$A_6^{(0)}(gg \rightarrow gggg)$$



$$A_5^{(1)}(gg \rightarrow ggg)$$



$$A_4^{(2)}(gg \rightarrow gg)$$

[Berends, Giele '87], [Mangano, Parke, Xu '87], [Britto, Cachazo, Feng '06]

[Bern, Dixon, Kosower '93]

[Anastasiou, Glover, Oleari, Tejeda-Yeomans '01],[Bern, De Freitas, Dixon '02]

$$d\hat{\sigma}_{NNLO} = \int_{d\Phi_4} d\hat{\sigma}_{NNLO}^{RR} + \int_{d\Phi_3} d\hat{\sigma}_{NNLO}^{RV} + \int_{d\Phi_2} d\hat{\sigma}_{NNLO}^{VV}$$

- explicit infrared poles from loop integrations
- implicit poles in phase space regions for single and double unresolved gluon emission
- procedure to extract the infrared singularities and assemble all the parts in a parton-level generator
- differential cross sections → kinematics of the final state intact to apply arbitrary phase space observable cuts

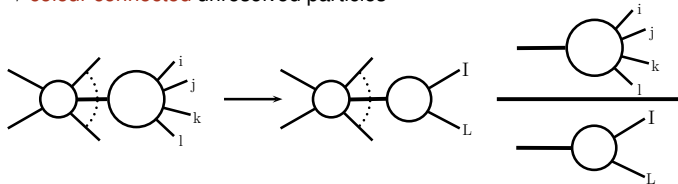
NNLO antenna subtraction

$$\begin{aligned} d\hat{\sigma}_{NNLO} &= \int_{d\Phi_4} \left(d\hat{\sigma}_{NNLO}^{RR} - d\hat{\sigma}_{NNLO}^S \right) \\ &+ \int_{d\Phi_3} \left(d\hat{\sigma}_{NNLO}^{RV} - d\hat{\sigma}_{NNLO}^T \right) \\ &+ \int_{d\Phi_2} \left(d\hat{\sigma}_{NNLO}^{VV} - d\hat{\sigma}_{NNLO}^U \right) \end{aligned}$$

- $d\hat{\sigma}_{NNLO}^S$: real radiation subtraction term for $d\hat{\sigma}_{NNLO}^{RR}$
- $d\hat{\sigma}_{NNLO}^T$: one-loop virtual subtraction term for $d\hat{\sigma}_{NNLO}^{RV}$
- $d\hat{\sigma}_{NNLO}^U$: two-loop virtual subtraction term for $d\hat{\sigma}_{NNLO}^{VV}$
- subtraction terms constructed using the **antenna subtraction method** at NNLO for **hadron colliders** → presence of **initial state** partons to take into account
- contribution in each of the round brackets is **finite**, well behaved in the **infrared singular regions** and can be evaluated **numerically**

NNLO antenna subtraction

- universal factorisation of both colour ordered matrix elements and the $(m+2)$ - particle phase space → colour connected unresolved particles



$$|M_{m+4}(\dots, i, j, k, l, \dots)|^2 J(\{p_{m+4}\}) \longrightarrow |M_{m+2}(\dots, I, L, \dots)|^2 J(\{p_{m+2}\}) \cdot X_4^0(i, j, k, l)$$

- momentum map $\{p_i, p_j, p_k, p_l\} \rightarrow \{p_I, p_L\}$ enforces momentum conservation away from the unresolved limits
- phase-space factorisation

$$\begin{aligned} d\Phi_{m+2}(p_a, \dots, p_i, p_j, p_k, p_l, \dots, p_{m+2}) &= d\Phi_m(p_a, \dots, p_I, p_L, \dots, p_{m+2}) \\ &\quad d\Phi_{X_{ijkl}}(p_i, p_j, p_k, p_l) \end{aligned}$$

- integrated antennae is the inclusive integral

$$\mathcal{X}_{ijkl}^0(s_{ijkl}) = \frac{1}{C(\epsilon)^2} \int d\Phi_{X_{ijkl}}(p_i, p_j, p_k, p_l) X_4^0(i, j, k, l)$$

Antenna functions and types

- colour-ordered pair of hard partons (**radiators**) with radiation in between
 - hard quark-antiquark pair
 - hard quark-gluon pair
 - hard gluon-gluon pair
- three-parton antenna → **one unresolved parton**
 - can be at **tree level** or at **one loop**
- four-parton antenna → **two unresolved partons**
- can be **massless** or **massive**
- all have three antenna types
 - **final-final antenna**
 - **initial-final antenna**
 - **initial-initial antenna**
- all three-parton and four-parton antenna functions can be derived from physical matrix elements, normalised to two-parton matrix elements

Integrated antennae

- antennae integrals are performed once and for all to become **universal** building blocks for subtraction of IR **singularities** at NNLO
- massless antennae ($m = 0$)

	NLO	NNLO
final-final	\checkmark^1	\checkmark^1
initial-final	\checkmark^2	\checkmark^3
initial-initial	\checkmark^2	$\checkmark^{4,5,6}$

- [1] A. Gehrmann-De Ridder, T. Gehrmann and E. W. N. Glover, *JHEP* **09** (2005) 056 [[hep-ph/0505111](#)];
- [2] A. Daleo, T. Gehrmann and D. Maître, *JHEP* **04** (2007) 016 [[hep-ph/0612257](#)];

- [3] A. Daleo, A. Gehrmann-De Ridder, T. Gehrmann and G. Luisoni, *JHEP* **01** (2010) 118 [[0912.0374](#)];
- [4] R. Boughezal, A. Gehrmann-De Ridder and M. Ritzmann, *JHEP* **02** (2011) 098 [[1011.6631](#)];
- [5] T. Gehrmann, P.F. Monni, *JHEP* **12** (2011) 049 [[1107.4037](#)];
- [6] A. Gehrmann-De Ridder, T. Gehrmann and M. Ritzmann, *JHEP* **10** (2012) 047 [[1207.5779](#)];

NNLO antenna subtraction

Implementation checks $pp \rightarrow 2j$ at NNLO:

- subtraction terms correctly approximate the matrix elements in all unresolved configurations of partons j, k

$$d\hat{\sigma}_{NNLO}^{RR,RV} \xrightarrow{\forall \{j,k\}, \{j\} \rightarrow 0} d\hat{\sigma}_{NNLO}^{S,T}$$

- local (pointwise) **analytic cancellation** of all infrared explicit ϵ -poles when integrated subtraction terms are combined with **one, two-loop matrix elements**

$$\text{Poles} \left(d\hat{\sigma}_{NNLO}^{RV} - d\hat{\sigma}_{NNLO}^T \right) = 0$$

$$\text{Poles} \left(d\hat{\sigma}_{NNLO}^{VV} - d\hat{\sigma}_{NNLO}^U \right) = 0$$

- leading and subleading colour
- process independent NNLO subtraction scheme
- allows the computation of **multiple differential distributions** in a single program run

Jet production partonic channels

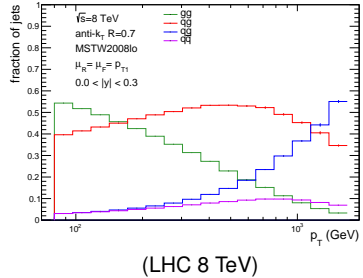
Fraction of jets per initial state contribution

LHC

- $gg \rightarrow gg$ dominates at low p_T
- $qg \rightarrow qg$ important in all p_T regions
- $qq \rightarrow qq$ dominant at high p_T

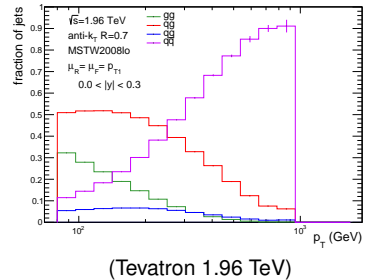
Tevatron

- qg and $q\bar{q}$ dominant



Present results at NNLO for

- $gg \rightarrow gg$ at leading colour
- $gg \rightarrow gg$ at subleading colour
- $q\bar{q} \rightarrow gg$ at leading colour

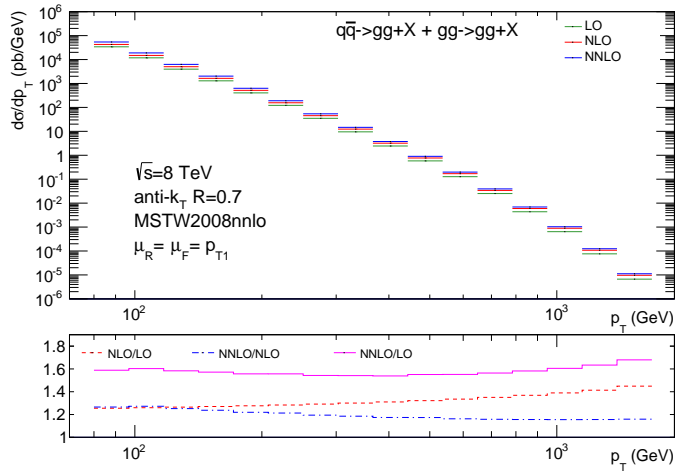


Numerical setup

(J.Currie, A. Gehrmann-De Ridder, T.Gehrmann, N. Glover, JP '13)

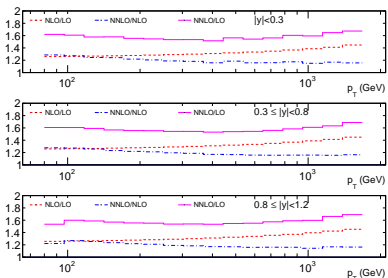
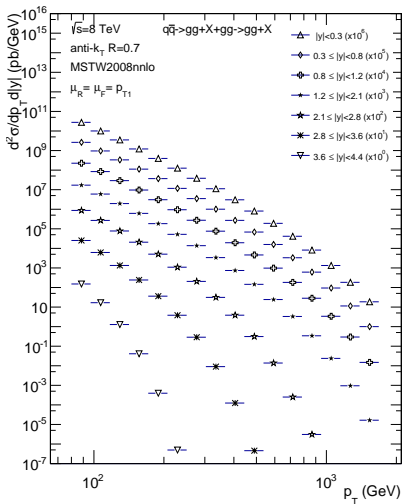
- pp collisions at $\sqrt{s} = 8$ TeV
- jets identified with the anti- k_T jet algorithm with resolution parameter $R = 0.7$
- jets accepted at rapidities $|y| < 4.4$
- leading jet with transverse momentum $p_T > 80$ GeV
- subsequent jets required to have at least $p_T > 60$ GeV
- MSTW2008nnlo PDF for all fixed-order predictions
- dynamical factorization and renormalization scales equal to the leading jet p_T
 $(\mu_R = \mu_F = \mu = p_{T1})$
- present results for full colour $gg \rightarrow gg$ scattering and $q\bar{q} \rightarrow gg$ leading colour combined at NNLO

Inclusive jet p_T distribution at NNLO



- all jets in an event are binned
- NNLO correction stabilizes the NLO k-factor growth with p_T
- NNLO corrections 15 – 26% with respect to NLO

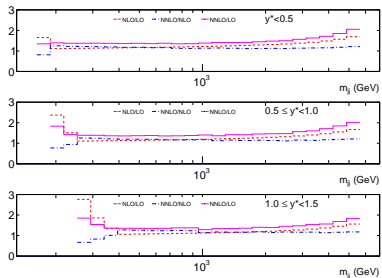
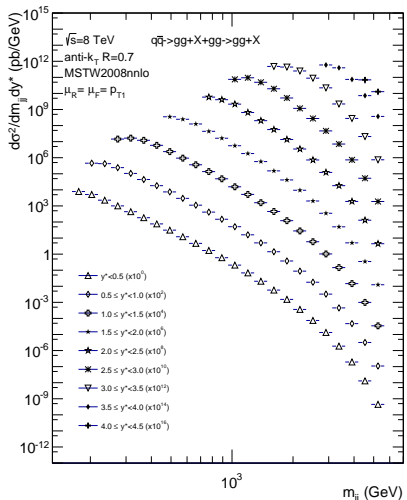
Double differential inclusive jet p_T distribution at NNLO



double differential k-factors

- NNLO prediction increases between 25% to 15% with respect to the NLO cross section
- similar behaviour between the rapidity slices

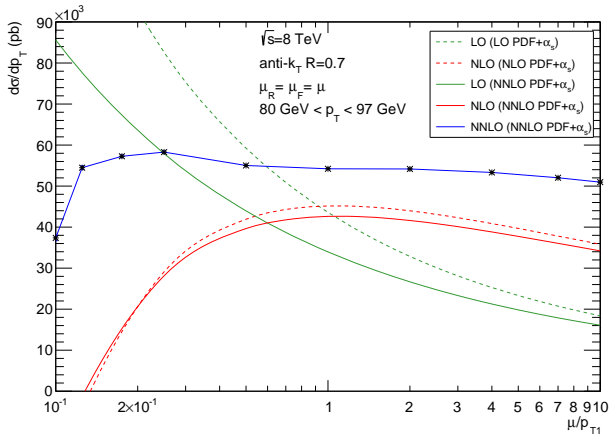
Double differential exclusive dijet mass distribution at NNLO



double differential k-factors

- NNLO corrections up to 20% with respect to the NLO cross section
- similar behaviour between the $y^* = 1/2|y_1 - y_2|$ slices

Inclusive jet p_T scale dependence ($gg \rightarrow gg + X$)



- scale dependence study gluons only $N_F = 0$ channel at leading colour
- dynamical scale choice: leading jet p_{T1}
- flat scale dependence at NNLO

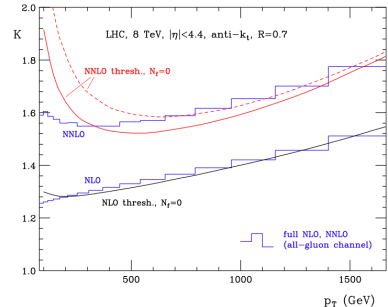
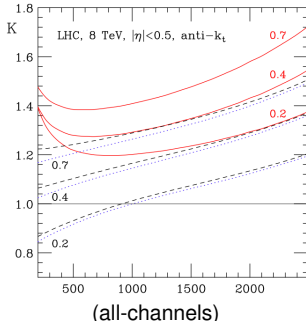
Threshold resummation approximation to exact NNLO

- Approximate NNLO results from an improved threshold calculation for the single jet inclusive production

[de Florian, Hinderer, Mukherjee, Ringer, Vogelsang '13]

- $pp \rightarrow j + X$ with the **threshold limit** given by $s_4 = P_X^2 \rightarrow 0$
- near **threshold** phase space available for **real-gluon** emission is **limited**
- higher k th order coefficient functions dominated by **large logarithmic corrections**

$$\alpha_s^k w_{ab}^{(k)} \rightarrow \alpha_s^k \left(\frac{\log^m(z)}{z} \right)_+, \quad m \leq 2k-1, \quad z = \frac{s_4}{s}$$



(gluons only channel) - rapidity integrated

NNLO benchmark predictions for jet production

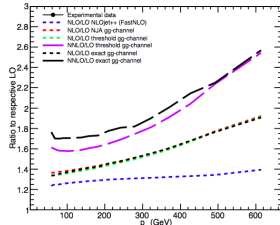
S. Carrazza, JP (*in preparation*)

- understand and characterise the validity of the NNLO threshold approximation by comparing it with the exact computation using the gg -channel
- comparison performed differential in p_T and rapidity following the exact experimental setups
- NNPDF23_nnlo_as_0118 set for all fixed order predictions
- NLO benchmark curves
 - green dashed curves → NLO-threshold gg -channel
 - black dashed curves → NLO-exact gg -channel
 - blue dashed curves → NLO-exact all channels
- NNLO benchmark curves
 - pink long-dashed curves → NNLO-threshold gg -channel → $d\sigma_{gg,NNLO}^{\text{thresh}} / d\sigma_{gg,LO}$
 - black long-dashed curves → NNLO-exact gg -channel → $d\sigma_{gg,NNLO}^{\text{exact}} / d\sigma_{gg,LO}$

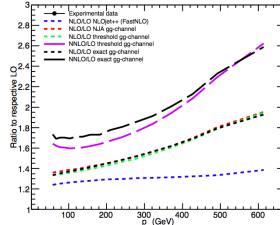
Tevatron CDF Run-II $\sqrt{s}=1.96$ TeV

S. Carrazza, JP (*in preparation*)

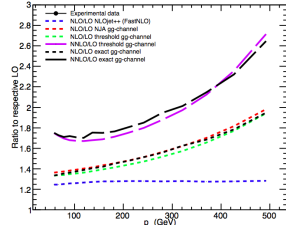
K-Factors - CDF Run-II kt, $|\eta|<0.1$



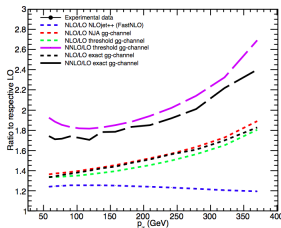
K-Factors - CDF Run-II kt, $0.1<|\eta|<0.7$



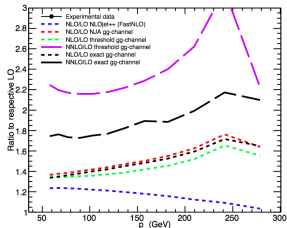
K-Factors - CDF Run-II kt, $0.7<|\eta|<1.1$



K-Factors - CDF Run-II kt, $1.1<|\eta|<1.6$



K-Factors - CDF Run-II kt, $1.6<|\eta|<2.1$

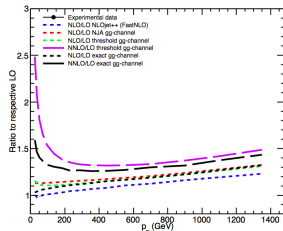


- differences $\leq 15\%$ at low- p_T in the central regions
- in the forward region differences $\geq 40\%$ for all p_T regions

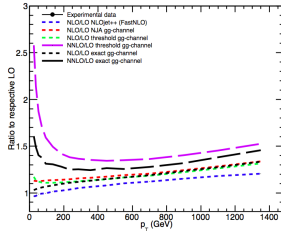
LHC ATLAS 2010 $\sqrt{s}=7$ TeV

S. Carrazza, JP (*in preparation*)

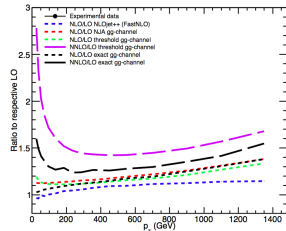
K-Factors - ATLAS 2010 7 TeV, $|\eta|<0.3$



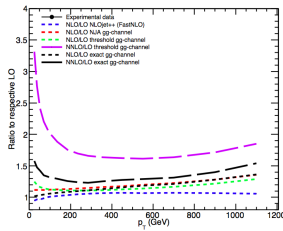
K-Factors - ATLAS 2010 7 TeV, $0.3<|\eta|<0.8$



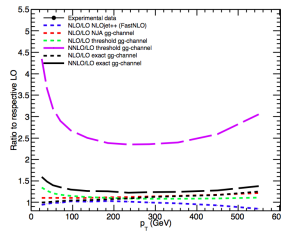
K-Factors - ATLAS 2010 7 TeV, $0.8<|\eta|<1.2$



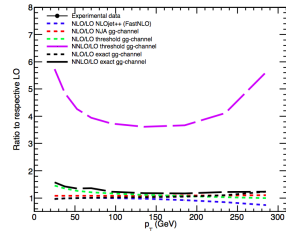
K-Factors - ATLAS 2010 7 TeV, $1.2<|\eta|<2.1$



K-Factors - ATLAS 2010 7 TeV, $2.1<|\eta|<2.8$



K-Factors - ATLAS 2010 7 TeV, $2.8<|\eta|<3.6$



- differences large at small p_T and increase with rapidity
- exact NNLO k-factor decreases with rapidity, NNLO threshold k-factor increases with rapidity

Conclusions

- antenna subtraction method generalised for the calculation of NNLO QCD corrections for exclusive collider observables with partons in the initial-state
- explicit ϵ -poles in the matrix elements are analytically cancelled by the ϵ -poles in the subtraction terms
- non-trivial check of analytic cancellation of infrared singularities between double-real, real-virtual and double-virtual corrections
- successful inclusion of subleading colour contributions at NNLO with the antenna subtraction method
- first exact results for $gg \rightarrow gg + X$ and $q\bar{q} \rightarrow gg + X$ at NNLO
- performed comparison between exact NNLO results and approximate NNLO results from threshold resummation in the gg -channel
 - largest differences arise at low- p_T for central rapidities and all p_T at large rapidities
 - differences are smaller at the Tevatron than at the LHC 7 TeV

Future work:

- include remaining channels involving the quark contributions
 - qg channel - most important at the LHC
 - leading colour N_F pieces
 - qq channel - important at high p_T

Back-up slides

QCD cross sections at subleading color beyond NLO

(J.Currie, A. Gehrmann-De Ridder, N. Glover, JP '13)

- **subleading colour matrix elements** have **incoherent interferences**, gluon scattering

$$|\mathcal{M}_6^0|^2 = g^8 N^4 (N^2 - 1) \sum_{\sigma \in S_6 / Z_6} \left[|A_6^{(0)}(\sigma)|^2 + \frac{2}{N^2} A_6^0(\sigma) \left(A_6^{\dagger 0}(\sigma') + A_6^{\dagger 0}(\sigma'') + A_6^{\dagger 0}(\sigma''') \right) \right]$$

- **one-loop five parton matrix elements**, gluon scattering

$$2\Re \left(\mathcal{M}_5^0 \mathcal{M}_5^{\dagger 1} \right) = g^8 N^4 (N^2 - 1) \sum_{\sigma \in S_5 / Z_5} 2\Re \left[A_5^{\dagger 0}(\sigma) A_5^1(\sigma) + \frac{12}{N^2} A_5^{\dagger 0}(\sigma) A_{5,1}^1(\sigma') \right]$$

- $\sigma', \sigma'', \sigma'''$ have **no common neighbouring partons** with σ

⇒ no single, double or triple collinear singularities at subleading colour ✓

- subtract **divergences** associated with **single** and **double soft gluons** only which at **subleading colour** map completely to the **tree-level single soft gluon current** $\rightarrow X_3^0$ **tree level three parton antenna**